

Germyl Wright–West Anionic Migration. Ab Initio Theoretical Study of the Reaction Mechanism in the Case of a Free Anion

Paola Antoniotti[†] and Glauco Tonachini^{*,‡}

Dipartimento di Chimica Generale ed Organica Applicata and Istituto di Chimica Organica della Università di Torino, via Pietro Giuria 7, I-10125 Torino, Italy

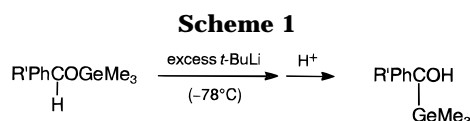
Received June 22, 1995[⊗]

The mechanism of the nondissociative [1,2] germyl rearrangement in the $(\text{H}_2\text{COGeH}_3)^-$ model system appears to be significantly different from its silicon analogue. A first exothermic step leads quite easily ($\Delta E^\ddagger = 2 \text{ kcal mol}^{-1}$) to a flat zone on the energy hypersurface, corresponding to a cyclic arrangement of the C, O, and Ge atoms, in which Ge is pentacoordinate. However, this kind of structure (ca. 12 kcal mol^{-1} below the carbanion; 18 kcal mol^{-1} for silicon) is unstable with respect to ring opening to the final oxyanion (for silicon the cyclic structure is stable). The overall migration is exothermic by 32 kcal mol^{-1} (only 20 kcal mol^{-1} for silicon). At variance with silicon, the importance of a cyclic intermediate is thus quite dubious in the germanium case. This result can explain the experimentally observed absence of products originating from the open-chain carbanion, when the migrating system is exposed to an electrophile. Finally, the energy barrier for oxygen–germanium bond cleavage is found to be ca. 10 kcal mol^{-1} : therefore, the dissociative process is not likely to be significantly competitive with the direct [1,2] shift.

Introduction

Twenty years ago Wright and West studied the anionic rearrangements of different silyl and germyl groups on carbon–oxygen or carbon–sulfur skeletons, taking place in the presence of excess strong base.^{1–3} This migration results in the transformation of a silyl or germyl ether (or sulfide) into its isomeric alcohol (or thiol) and is therefore the silicon or germanium analogue of the well-known Wittig rearrangement,⁴ in which the carbon-centered migrating moiety is an alkyl, aryl or allyl group. In Scheme 1 the germanium rearrangement studied by Wright and West in refs 1 and 3 is shown ($R' = \text{H}$ or Ph). When the base is present only in catalytic amounts, the reverse migration (whose mechanism must be closely related) takes place, which is called anti-Wittig or Brook rearrangement.⁵

The theoretical study of the silicon Wright–West reaction was recently undertaken, by studying the silyl migration from oxygen to carbon in the simple H_2COSiH_3 free anion⁶ and its lithiated counterpart.⁷ In the present study, the behavior of the similar germa-



num system will be explored, with the purpose of inspecting similarities and differences with respect to its silicon analogue. It was indeed observed experimentally¹ that the rearrangements shown in Scheme 1 take place very easily, suggesting to the authors that “germanium, like silicon, can form low-energy pentacoordinate transition states” (ref 1, pp 3218 and 3219). However, some interesting differences were stressed at the same time. Namely, both metalated germyl ethers shown in Scheme 1 were observed to react slowly with methyl iodide (in contrast with the behavior of the similar silicon anions), giving only the rearranged system $\text{R}'\text{PhC}(\text{GeMe}_3)\text{O}-\text{Me}$ and suggesting that little or no carbanion was present.

In the present study, the gas-phase energy profile for the direct migration of the germyl group in the free anion is first defined, with the main purpose of establishing if the intervention of a cyclic pentacoordinated-germanium intermediate can be soundly postulated (this was the more outstanding feature of the silicon rearrangement).⁶ Then a dissociative process, involving the cleavage of the $\text{Ge}-\text{O}$ bond is considered (in the case of silicon this pathway was not competitive with the direct shift). Two other aspects of the problem, neglected in the present paper, will deserve further investigation: (i) the extent to which a differential stabilization operated by lithium on the structures of chemical interest can affect the reaction energetics and possibly the description of the mechanism; (ii) the role of substituents on the negative carbon in affecting the qualitative description of the mechanisms discussed in the present paper for germanium and in ref 6 for silicon.

[†] Dipartimento di Chimica Generale ed Organica Applicata.

[‡] Istituto di Chimica Organica.

[⊗] Abstract published in *Advance ACS Abstracts*, January 15, 1996.

(1) Wright, A.; West, R. *J. Am. Chem. Soc.* **1974**, *96*, 3214–3222.

(2) Wright, A.; West, R. *J. Am. Chem. Soc.* **1974**, *96*, 3222–3227.

(3) Wright, A.; West, R. *J. Am. Chem. Soc.* **1974**, *96*, 3227–3232.

(4) Wittig, G.; Lohmann, L. *Ann. Chim.* **1942**, *550*, 260–268. Wittig, G. *Angew. Chem.* **1954**, *66*, 10–17.

(5) Brook, A. G.; Legrow, G. E.; MacRae, D. M. *Can. J. Chem.* **1967**, *45*, 239–253. Brook, A. G.; Warner, C. M.; Limburg, W. W. *Can. J. Chem.* **1967**, *45*, 1231–1246. Brook, A. G. *Acc. Chem. Res.* **1974**, *7*, 77–84. For a recent experimental paper dealing with the Brook rearrangement (in which kinetic and stereochemical results are discussed) see: Reich, H. J.; Holtan, R. C.; Bolm, C. *J. Am. Chem. Soc.* **1990**, *112*, 5609–5617.

(6) Antoniotti, P.; Tonachini, G. *J. Org. Chem.* **1993**, *58*, 3622–3632.

(7) Antoniotti, P.; Canepa, C.; Tonachini, G. *J. Org. Chem.* **1994**, *59*, 3952–3959.

Methods

The study of the rearrangement reaction was performed by determining on the energy hypersurface the critical points relevant to stable and transition structures. This was initially accomplished by way of complete gradient optimization⁸ of the geometrical parameters at the Hartree–Fock (HF) level of theory, using the split-valence shell 3-21+G(*) basis set⁹ (diffuse sp functions on all non-hydrogen atoms and d polarization functions centered on germanium only). The critical points relevant to the [1,2] migration process were characterized at this level as minima or first-order saddle points, through diagonalization of the analytically calculated Hessian matrix (vibrational frequencies calculation). Following this first exploration of the reaction surface, MP2¹⁰ optimizations were carried out with the more flexible split-valence shell spd basis set by Huzinaga and co-workers, enriched with diffuse p functions and d polarization functions on all non-hydrogen atoms (this computational level will be denoted as MP2/[552/331/2] in the following).¹¹ The energy profile for the direct shift was redefined by recomputing the relative energies through perturbative MP4¹⁰/[552/331/2] calculations. The O–Ge bond cleavage transition structure from the initial carbanion was determined by CAS-MCSCF¹²/[552/331/2] calculations involving three active orbitals and four electrons in the active space (see details in the following section); then, in order to define the nature of the wave function along a dissociation profile, a whole series of CAS-MCSCF/[552/331/2] geometry optimizations at fixed O–Ge distances was performed. The analysis of these results allowed us to get, in a further step, an approximate energy profile homogeneous with that computed for the nondissociative process, by using all CAS-MCSCF/[552/331/2] geometries to recompute the relative energies at the MP4/[552/331/2] level. The electron distribution for the [1,2] migration process is discussed in terms of NAO charges and NBO analysis.¹³ In the figures of the following section the reported interatomic distances are in angstroms, and angles, in degrees; dihedral angles are reported in parentheses (plain

(8) Schlegel, H. B. In *Computational Theoretical Organic Chemistry*, Csizsmaia, I. G., Daudel, R., Eds.; Reidel Publ. Co.:Dordrecht, The Netherlands, 1981; p 129. Schlegel, H. B. *J. Chem. Phys.* **1982**, *77*, 3676–3681. Schlegel, H. B.; Binkley, J. S.; Pople, J. A. *J. Chem. Phys.* **1984**, *80*, 1976–1981. Schlegel, H. B. *J. Comput. Chem.* **1982**, *3*, 214.

(9) Binkley, J. S.; Pople, J. A.; Hehre, W. J. *J. Am. Chem. Soc.* **1980**, *102*, 939–947; Clark, T.; Chandrasekhar, J.; Schleyer, P. v. R. *J. Comput. Chem.* **1983**, *4*, 294. Dobbs, K. D.; Hehre, W. J. *J. Comput. Chem.* **1986**, *7*, 359–378.

(10) Møller, C.; Plesset, M. S. *Phys. Rev.* **1934**, *46*, 618. Binkley, J. S.; Pople, J. A. *Int. J. Quantum Chem.* **1975**, *9*, 229–236. Pople, J. A.; Binkley, J. S.; Seeger, R. *Int. J. Quantum Chem. Symp.* **1976**, *10*, 1–19. Krishnan, R.; Pople, J. A. *Int. J. Quantum Chem. Symp.* **1980**, *14*, 91. Restricted MP2 geometry optimizations were run within the “frozen core approximation”, while single-point restricted MP4 calculations were carried out without frozen orbitals, by considering single, double, triple, and quadruple excitations (using the “full” and “SDTQ” options¹⁴); this computational level is simply referred to as MP4 in the text. Six Cartesian d functions were employed throughout.

(11) Huzinaga, S.; Andzelm, J.; Klobukowski, M.; Radzio-Andzelm, E.; Sakai, Y.; Tatewaki, H. *Gaussian Basis Sets for Molecular Calculations*. In *Physical Sciences Data 16*; Elsevier: Amsterdam, 1984. For Ge/Si/C and O/H, the basis consists of (13s, 11p, 5d/11s, 9p, 1d/7s, 5p, 1d/4s) Gaussians, respectively, which are grouped as follows: 43321 (s), 43211 (p), and 41 (d) for Ge (the last p is the diffuse set; the second d, the polarization set); 4331 (s), 4311 (p, the last one a diffuse function), and 1 (d, the polarization set) for Si; 421 (s), 311 (p), and 1 (d) for C, O (the last p is the diffuse set; the single d is the polarization set); 31 for H. This provides a [552/441/331/2] basis set. Therefore, polarization d functions are present on non-hydrogen atoms, as well as diffuse p functions. The exponents of the latter were taken from: Dunning, T. H.; Hay, P. J. *Methods of Electronic Structure Theory*. In *Modern Theoretical Chemistry*; Schaefer, H. F., III, Ed.; Plenum Press: New York and London, 1977; Vol. 3, Chapter 1. For Ge, the diffuse p function exponent was set to 0.045, on the basis of an optimization on the germlyl anion.

(12) Robb, M. A.; Eade, R. H. A. *NATO Adv. Study Inst. Ser.* **1981**, *C67*, 21.

(13) Reed, A. E.; Weinstock, R. B.; Weinhold, F. *J. Chem. Phys.* **1985**, *83*, 735–746. Reed, A. E.; Weinhold, F. *J. Chem. Phys.* **1983**, *78*, 4066–4073. Foster, J. P.; Weinhold, F. *J. Am. Chem. Soc.* **1980**, *102*, 7211–7218.

figures, RHF values; bold, MP2 values; italic, CAS-MCSCF values). The GAUSSIAN92 system of programs¹⁴ was used throughout, on IBM RISC/6000 computers.

Results and Discussion

Nondissociative Pathway. The gas-phase energy profile for a direct migration of the germlyl group from oxygen to carbon has first been defined. Germlyloxymethanide (Figure 1a) is the model “reactant”. In **1a** the lone pair on carbon is antiperiplanar with respect to the O–Ge bond; this conformation could be labeled for convenience as “W”, from the position of germanium relative to the two methylenic hydrogens in a Newman projection. Any attempt to locate a “Y” conformational minimum, in which the methylenic group is rotated by 180° and the lone pair on carbon is synperiplanar to the O–Ge bond, failed, because ring closure with formation of a Ge–C bond occurred very readily, without any energy barrier.

In Figure 1b,c two structures are shown, which correspond to first-order saddle points on the energy hypersurface (the analytically computed Hessian matrix has index 1). In **1b** germanium gets closer to the methylenic carbon atom, and CH₂ inversion occurs. The largest components of the transition vector (first eigenvector of the Hessian) are relevant to the two methylenic HCOX dihedral angles (0.69 and –0.69, respectively), coupled with the motion of the germlyl group almost parallel to the C–O bond (0.17 coefficient for the COGe angle). Thus, the geometrical parameters of **1b**, and the nature of the transition vector, show that this transition structure is related to the migration process. The energy barrier is 7 kcal mol^{–1} (Table 1).¹⁵ In Figure 1c, on the other hand, a methylene rotation transition structure is shown, in which the COGeH₃ part of the molecule is altered insignificantly with respect to **1a**. The transition vector is dominated again by the two methylene HCOX dihedral angles, this time with the same sign (0.69 and 0.72). This energy barrier is much smaller than the previous one (Table 1).¹⁵ Yet, some doubts could be cast on the importance of this transition structure, because of its dubious relevance to the migration process itself: actually, it more closely resembles a conformational transition structure. Moreover, if carbon and germanium are significantly closer in **1b** than in **1a** (the C–Ge distance has dropped from 2.915 (HF) or 2.773 Å (MP2) to 2.740 or 2.660 Å), **1c** is, from this point of view, closer to the reagent, and the C–Ge distance changes much less: 2.918 (HF) or 2.762 Å (MP2). However, as reported above, a Y conformation

(14) Frisch, M. J.; Trucks, G. W.; Head-Gordon, M.; Gill, P. M. W.; Wong, M. W.; Foresman, J. B.; Johnson, B. G.; Schlegel, H. B.; Robb, M. A.; Replogle, E. S.; Gomperts, R.; Andres, J. L.; Ragavachari, K.; Binkley, J. S.; Gonzales, C.; Martin, R. I.; Fox, D. J.; Defrees, D. J.; Baker, J.; Stewart, J. J. P.; Pople, J. A. *Gaussian Inc.*, Pittsburgh, PA, 1992 (GAUSSIAN92).

(15) The convergence of the perturbative series appears to be satisfactory, as can be seen from the MPn/[552/331/2] energy differences collected below. These can in turn be compared with the variational estimate reported in the last column (CISD energy corrected to fourth order: Pople, J. A.; Seeger, R.; Krishnan, R. *Int. J. Quantum Chem. Symp.* **1977**, *11*, 149).

	MP2	MP3	MP4	CISD
TS	1b 5.76	6.46	6.97	9.70
TS	1c 2.21	1.97	2.11	1.44
shoulder (C–x = 0.75)	2a –12.14	–10.66	–11.68	–9.86
oxyanion	2c –31.64	–31.39	–31.96	–32.15

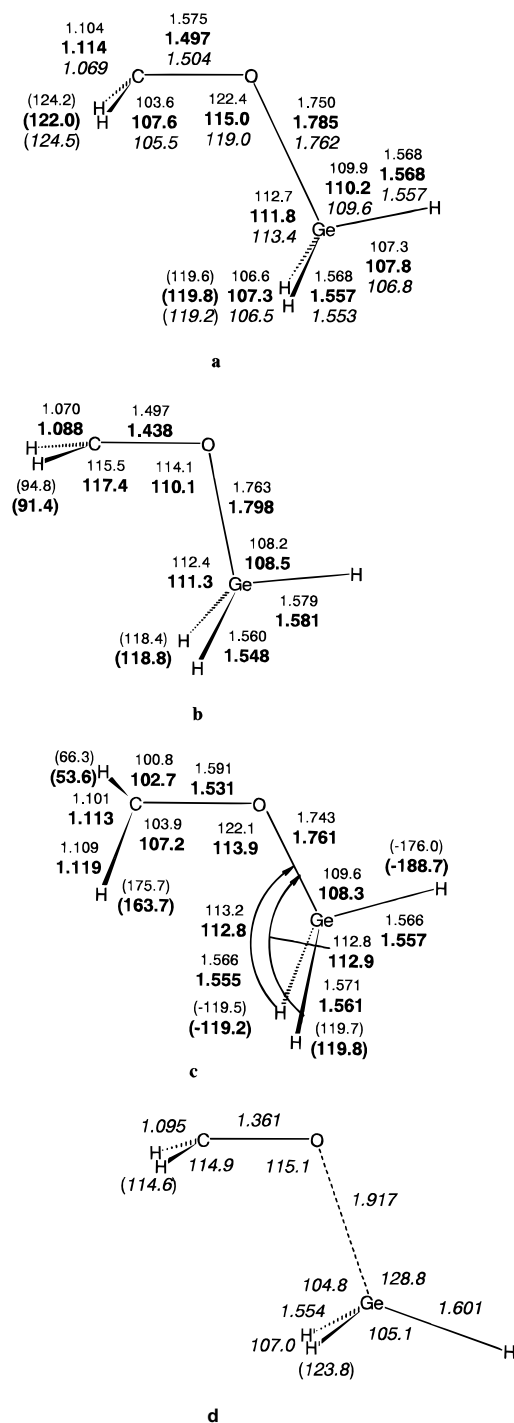


Figure 1. (a) Germoxymethanide (C_s). (b) CH_2 -inversion transition structure (C_s). CH_2 -hydrogen dihedral angles refer to a dummy center X, bound to C and anti to Ge; those relevant to germyl out-of-plane hydrogens refer to the in-plane H. (c) CH_2 -rotational transition structure (C_1). GeH_3 dihedral angles are defined, for the rightmost hydrogen H' , as $H'GeOC$, and, for the two remaining hydrogens, as $HGeOH'$. (d) Transition structure for dissociation of (a) into two fragments.

of the reactant does not exist. Hence, a methylene rotation can open a viable pathway toward ring closure, even if the initial part of this pathway is almost orthogonal (in the coordinate space) to a migration motion. These two transition structures are reminiscent of those found in the case of the silicon free anion (ref 6, structures **1b,c**); the barriers too have similar height. All of these structures potentially lead to direct ring

closure. The stereochemical outcome of a reaction involving a negative carbon bearing two different groups would of course depend on which pathway is preferred, and from the present results the second pathway comes out to be clearly preferred. However, the results collected for the silicon migration, in the presence and absence of a lithium counterion,^{6,7} suggest that the stereochemistry of the migration process can depend to some extent on the degree of cation–anion association. This aspect of the mechanism will be addressed in a follow-up study.

In the preliminary $HF/3-21+G^*$ exploration, a penta-coordinate-germanium cyclic intermediate could be easily obtained from either **1b** or **1c**: at this level, it corresponds to a well-defined minimum on the energy hypersurface (Figure 2a).^{16a} An important feature of the silicon free anion rearrangement⁶ would thus be found also for the analogue germanium system. However, $MP2/[552/331/2]$ optimization attempts do not yield a well-defined minimum. In fact, a series of constrained optimizations, in correspondence of fixed values of the C–x parameter (see Figure 2a), allowed to define a shoulder zone (see Table 2).¹⁷ The optimum geometrical parameters of the structure corresponding to the value C–x = 0.75, representative of this zone, are reported in Figure 2a. Although this geometry does not obviously belong to a critical point, it can be observed that in correspondence of **2a** the gradient is quite close to zero, in terms of the usual thresholds.¹⁷ Structure **2a** is thermodynamically and kinetically stable with respect to the original carbanion: the backward process, i.e. ring opening to **1a**, would require 13.8 kcal mol⁻¹. But it is not so with respect to the final oxyanion: indeed Ge migration (as expressed by further C–x shortening) can proceed without any energy barrier, and germyl rotation appears to take place very easily.

Consistently, a transition structure for GeH_3 rotation coupled with ring opening (Figure 2b) is found only at the $HF/3-21+G^*$ level.^{16b} It must be pointed out, however, that the two sets of data are not in sharp contrast, because the HF energy barrier separating **2a** from **2c** is in fact tiny, 0.4 kcal mol⁻¹. Thus, any unconstrained $MP2/[552/331/2]$ energy minimization from structures relevant to the shoulder zone converged smoothly on the final oxyanion, germylmethoxide, which is shown in Figure 2c. This result is opposed to that obtained for the silicon free anion,⁶ where a second stable conformation of the cyclic intermediate (having

(16) (a) $MP2/3-21+G^*$ calculations gave the same result of the HF calculations (the geometries are not reported). In the cyclic structure **2a** the arrangement of the various atoms around germanium can be thought of as a distorted trigonal bipyramid: the longer bonds can be associated with quasi-axial positions (C–Ge and in-plane Ge–H), the shorter to quasi-equatorial positions (O–Ge and the other two Ge–H bonds). (b) The transition vector in **2b** is dominated by the rotation of the GeH_3 group (the relevant dihedral angle coefficient is 0.75) coupled with a motion of Ge parallel to the C–O bond (coefficient 0.51). This motion leads to an exchange of axial and equatorial positions around germanium: $MP2/3-21+G^*$ calculations are again in accord with the HF ones, but the barrier reduces to only 0.1 kcal mol⁻¹. From the chemical point of view the disagreement between the two sets of $MP2$ computations does not appear to be particularly significant. All results obtained cast strong doubts on the very existence of a stable cyclic intermediate; even if it were weakly bound, such a structure would bear little chemical significance.

(17) These optimizations produced the energies E_{MP2} (–2189.xxxxxx; the decimal figures only are reported in Table 2), and the residual force along C–x, f_{Cx} . The $MP4/MP2$ energies used to draw the plot of Figure 3 are also reported (E_{MP4} , –2189.xxxxxx). Energy differences are relative to **1a**.

Table 1. Direct [1,2] Shift: Total^a and Relative^b Energies of the Critical Points

structure		MP4/[552/331/2] ^c		MP2/[552/331/2]		RHF/3-21+G(*)	
		<i>E</i>	ΔE	<i>E</i>	ΔE	<i>E</i>	ΔE
"W" carbanion	1a	-2189.361 901	0.0	-2189.289 329	0.0	-2180.462 809	0.0
TS (CH ₂ inv)	1b	-2189.350 794	7.0	-2189.279 977	5.9	-2180.449 754	8.2
TS (CH ₂ rot)	1c	-2189.358 531	2.1	-2189.285 886	2.2	-2180.461 572	0.8
cyclic struct	2a	-2189.380 516 ^d	-11.7	-2189.308 040 ^d	-11.7	-2180.478 529	-9.9
TS (ring opening)	2b					-2180.477 914	-9.5
oxyanion	2c	-2189.412 838	-32.0	-2189.339 347	-31.4	-2180.498 580	-22.4

^a Hartrees. ^b kcal mol⁻¹. ^c Computed at the MP2/[552/331/2] geometries of the critical points. ^d A shoulder point corresponding to C-x = 0.75 Å (see text and ref 17).

Table 2. Energy Data Relevant to the Shoulder Zone

	C-x						
	0.65	0.70	0.75	0.80	0.85	0.95	1.00
<i>E</i> _{MP4}	0.380859	0.380666	0.380516	0.380372	0.380204	0.379708	0.379353
ΔE _{MP4}	-11.90	-11.78	-11.68	-11.59	-11.49	-11.17	-10.95
<i>E</i> _{MP2}	0.308258	0.308130	0.308040	0.307953	0.307836	0.307413	0.307079
ΔE _{MP2}	-11.88	-11.80	-11.74	-11.69	-11.61	-11.35	-11.14
<i>f</i> _{Cx}	-0.00170	-0.00108	-0.00086	-0.00102	-0.00150	-0.003081	-0.00400

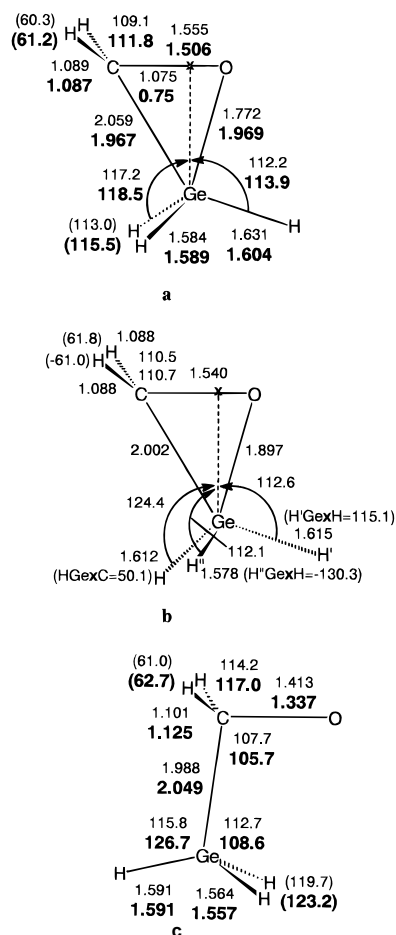


Figure 2. (a) Cyclic structure (C_s). MP2 values refer to a noncritical point representative of the shoulder zone (see text and ref 17). (b) GeH₃-rotational transition structure (C₁) leading to the oxyanion c. (c) Germylmethoxide (C_s). Dihedral angles are as in Figure 1.

the silyl group rotated by 180° with respect to the more stable conformation) was reachable through a transition structure similar to **2b**. Also a series of MP4[552/331/2] single-point computations (carried out using the MP2-[552/331/2] geometries for the shoulder zone) gave the result that no energy barrier appears to separate this region from the final oxyanion. All the results just discussed indicate that a stable cyclic intermediate is

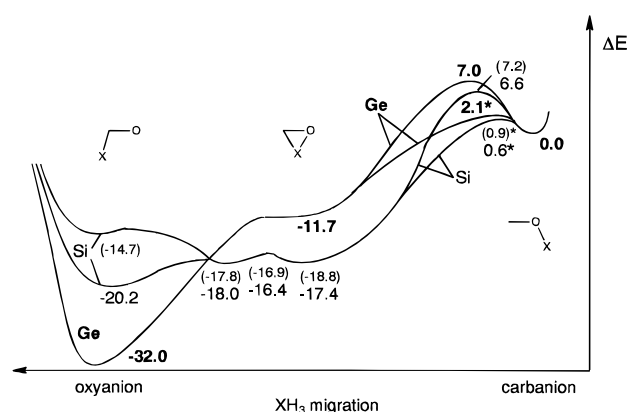


Figure 3. MP4/[552/331/2]/MP2/[552/331/2] energy profile for the germyl nondissociative shifts, along a symbolic reaction coordinate (bold figures). The analogous energy profile is shown for silyl migration, as taken from ref 6 (smaller figures in parentheses) or recomputed (see text).

not likely to exist. The second stage¹⁸ of the rearrangement, from the shoulder zone to the final oxyanion, is exothermic by ca. 20 kcal mol⁻¹ (the last step of the silicon rearrangement, leading to the oxyanion, was slightly endothermic).⁶

The overall rearrangement can be seen, similarly to the silicon case, as a nucleophilic displacement at germanium. In the first stage, carbon is the incoming nucleophile, whereas in the second stage oxygen is the leaving group. O⁻ in itself is not a good nucleofuge indeed; however, this step shows a significant exothermicity, which can be traced back to the obvious energy gain related to the carbanion-oxyanion transformation. However, this factor should have approximately the same weight for the silicon and germanium systems. In order to compare more homogeneous energy values, MP4[441/331/2]¹¹ single-point computations were carried out using the geometries of ref 6, relevant to the silicon rearrangement. It can be noted (Figure 3) that the exothermicity is affected by the change in computational level: the originally computed⁶ 15 kcal mol⁻¹

(18) This word is used as a descriptor of the sequence of variations in the main geometrical parameters within a single kinetic step, which appears to take place in two phases, due to the presence of the shoulder zone. Thus, on the basis of the higher quality calculations, this reaction appears to be a "one step/two stages" process.

becomes now 20 kcal mol⁻¹ (smaller in any case that that computed for the germanium system, 32 kcal mol⁻¹). This discrepancy sets the exothermicity difference between the Si and Ge reactions in the range 17–12 kcal mol⁻¹, in favor of the germanium system. Making reference to the values originally reported by Wright and West,¹ we can compare this computational result with the following approximate bond energies (in kcal mol⁻¹). In going from the carbanion to the oxyanion, one O–Ge bond (73) transforms into C–Ge (56), with a loss of 17; in going from O–Si (112) to C–Si (73), a loss of 39 is estimated. These losses can be thought of as superimposed to the mentioned indiscriminating energy gain. The change in bonding is thus less penalizing for the germanium system, by ca. 12 kcal mol⁻¹. This figure compares well with the computed exothermicity difference, which in summary can be attributed to the loss of stability related to the change in bonding situation, smaller in the germanium system and larger in its silicon analogue (compare the discussion in ref 1, p 3218). Besides, the exothermicity of the first stage in the germanium rearrangement is less pronounced than that relevant to the first step in the analogous silicon migration. From these results it can be obviously evinced that germanium is not as inclined as silicon to stay bound in a pentacoordinated cyclic arrangement. The overall features of the Ge and Si free anion rearrangements are summarized in the energy profiles reported in Figure 3 (the two starred energy difference values are relevant to CH₂ rotational transition structures, which should actually be represented along an axis orthogonal to the “migration” axis shown).

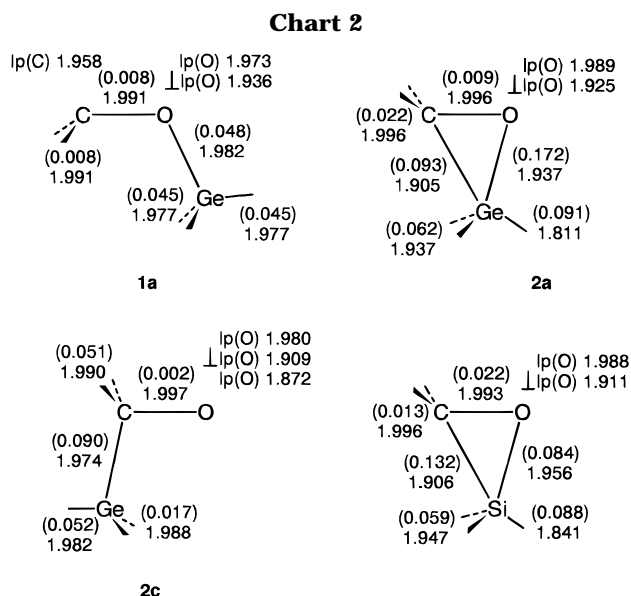
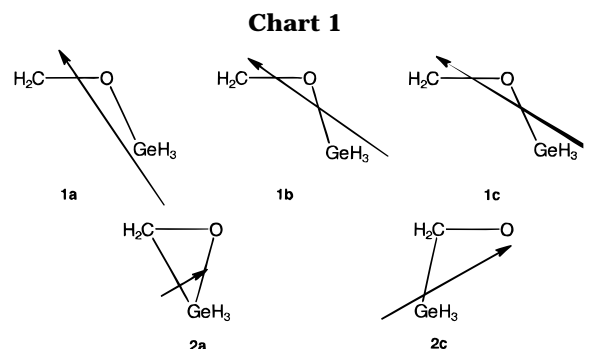
The results obtained for the silicon free anion,⁶ while providing the picture of an easy evolution of the initial carbanion into a cyclic intermediate (with an energy gain of ca. 18 kcal mol⁻¹), showed, in contrast with the present case, that two conformers of this intermediate can be considered in equilibrium and correspond to the lowest minima on the energy surface, while the open-chain oxyanion is 3–4 kcal mol⁻¹ higher in energy. In the germanium case it is reasonable to assume that proton abstraction brings about a rapid transformation of the initial open-chain structure into the final oxyanion, which should then be obtained quite readily. As a consequence, the initial carbanion will be virtually absent when the system will be eventually exposed to the action of a protonating agent or to any other electrophile. The silicon system, in contrast, could react at least partially through the cyclic intermediate, which could undergo ring opening with cleavage of either the C–Si or the O–Si bond. Moreover, making reference to the differences in reactivity between Si and Ge systems in the case of attack by MeI,¹ which were mentioned in the Introduction, it can be observed that the reacting moiety would be, in the silicon case, a strained cyclic intermediate;⁶ on the other hand, in the germanium case, the nucleophile would be the more stable oxyanion, presumably less inclined to react readily.¹⁹

Electron Distribution. The data presented in the following are based on the HF/[552/331/2] density (MP2

Table 3. Direct [1,2] Shift: NAO^a Group Charges^b and Dipole Moments^c

	$Q(\text{CH}_2)$	$Q(\text{O})$	$Q(\text{GeH}_3)$	μ
1a	-0.484	-0.983	0.466	9.55
1b	-0.517	-0.966	0.483	8.63
1c	-0.481	-1.012	0.494	8.78
2a	-0.242	-1.011	0.253	2.75
2c	-0.002	-1.023	0.024	6.02

^a NAO charges: see ref 13. ^b Group charges Q computed summing up C and H, or Ge and H, atomic charges at the RHF/[552/331/2] level. ^c Debye units.



geometries). In the open-chain free carbanion **1a** the charge is more localized on carbon, while in the “quasi intermediate” cyclic structure **2a**, representative of the shoulder zone, some redistribution of the electron density toward the germyl group has taken place and the charge is less localized. These changes in electron distribution are illustrated by the NAO group charges in Table 3. The charges can be compared with the orientation and lengths of the dipole moment vectors (Chart 1, Table 3). Concurrently, the energy of the HOMO is higher in the W carbanion **1a**, -0.044 H, than in the “quasi intermediate” **2a**, -0.099 H. The stretching of the Ge–H bonds from **1a** to **2a** suggests that this change in electron density distribution can be interpreted in terms of population of an initially empty molecular orbital with significant σ^*_{GeH} contributions, similar to silicon.⁶

Natural bond orbital analysis¹³ allows a description of the changes in bonding taking place when the anionic system evolves from **1a** to **2c**. In Chart 2 NBO populations are reported for **1a** and **2a,c**: populations of

(19) The counterion, if tightly bound, in **2c**, to the negative oxygen, could be expected to play an interesting role also in this case: it would presumably concur to completely rule out the “quasi-intermediate”, through differential stabilization of the open-chain structures, in which the charge is more localized.

Table 4. O–Ge Bond Dissociation: Energies^a and Energy Differences^b of the Critical Points^c

structure		MP4/[552/331/2] ^d		CAS-MCSCF/[552/331/2]	
		<i>E</i>	ΔE	<i>E</i>	ΔE
"W" carbanion	1a	-2189.357 781	0.0	-2188.863 865	0.0
dissociation TS	1d	-2189.340 569	10.8	-2188.848 458	9.7
heterolytic dissoc limit ^e		-2189.401 159	-27.2	-2188.934 125	-44.1
homolytic dissoc limit ^e		-2189.301 706	35.2	-2188.809 766	33.9

^a Hartrees. ^b kcal mol⁻¹. ^c CAS-MCSCF/[552/331/2] geometries. ^d Computed at the CAS-MCSCF/[552/331/2] geometries. ^e Geometrical parameters reported in ref 21.

antibonding NBO's are reported in parentheses, while those of lone pairs are marked "lp", with the oxygen lone pair perpendicular to the molecular plane marked " \perp lp". The main changes are of course relevant to the carbon lone pair in **1a**, which is involved in bond formation with germanium, and to the Ge–O bond in **2a**, which cleaves and transforms into an oxygen lone pair in **2c**. However the more interesting feature is, in **2a**, the declining of σ bond populations for all bonds centered on Ge, with respect to both open-chain structures, which is particularly significant for the in-plane σ_{GeH} bond. This drop is accompanied by a parallel increase in σ^* populations. Comparison with the data obtained at the same computational level for the more stable silicon cyclic intermediate (geometry from ref 6) shows that its bonding situation is very close to that of **2a**. The NBO populations just presented can be found to vary consistently with the changes in the more important geometrical variables.

Dissociative Process. A dissociation of the reacting system **1a** in two fragments, taking place by cleavage of the O–Ge bond and followed by reassociation through formation of a C–Ge bond, could in principle give the same product, **2c**, obtained through the nondissociative migration discussed above. This part of the study consists of two different phases. First, the nature of the wave function along a dissociative path was investigated by means of a series of CAS-MCSCF/[552/331/2] geometry optimizations carried out at fixed O–Ge distances, as well as by determining the optimum geometry of the transition structure for dissociation. Then, the analysis of the informations collected in the first phase allowed us to define a reaction profile homogeneous (as regards the energy computation) with that obtained for the nondissociative process, through a series of MP4/[552/331/2] single-point energy calculations on the CAS-MCSCF geometries.

The CAS-MCSCF active space chosen consists of those three orbitals which are more heavily involved in the dissociation process, populated by four electrons. These orbitals are, in the initial carbanion, the lone pair orbital, which is mainly localized on carbon (n_{C}), and the σ , σ^* couple of the O–Ge bond. This active space corresponds, for the separated fragments, to two orbitals belonging to the formaldehyde moiety (the π_{CO} , π^*_{CO} couple) and one belonging to the germyl fragment (the σ_{sp} orbital which involves the three hydrogens and is polarized away from them, σ_{GeH_3}). In this space a complete CI is performed and all molecular orbitals optimized.

First, the heterolytic and homolytic dissociation limits were determined by CAS-MCSCF/[552/331/2] geometry optimizations. In both cases a single configuration is clearly dominating in the CI eigenvector (coefficient larger than 0.98), indicating that recomputation of the energies at the (single reference) MP4 level is feasible

(Table 4). The heterolytic dissociation limit (corresponding to fragmentation into formaldehyde and germyl anion) is located quite low in energy with respect to **1a** at both levels, although the estimate provided by the two methods is different; in contrast, the homolytic (formaldehyde radical anion associated to a germyl radical) is at a much higher energy. In a comparison with the silicon case, the heterolytic dissociation limit is found to be much lower: there, it was estimated to lie at about the same energy as the carbanion, +1 kcal mol⁻¹.⁶ This result suggests that the reacting system **1a** could follow a viable dissociation-reassociation pathway, leading to the more stable fragments. This could be done, however, without necessarily attaining the dissociation limit, because the H₂CO and GeH₃ moieties can most likely be held together in an electrostatic complex: from this energy minimum, reassociation of the two molecules could then take place to give the product. In the case of silicon, the last part of the process was found to be very easy.⁶ For this reason, the investigation is limited here to the determination of the energy barrier for O–Ge bond dissociation, which is presumably the more difficult step.

In order to evaluate the energy barrier for dissociation, the initial carbanion was reoptimized at the CAS-MCSCF/[552/331/2] computational level (Figure 1a). The CI eigenvector is dominated by the aufbau configuration (0.993 coefficient), and the configuration corresponding to a double excitation from the first (σ_{OGe}) into the third (σ^*_{OGe}) active orbital is the second in order of importance (-0.114 coefficient). Consistently, the populations of the three active orbitals are 1.974, 2.000, and 0.026 electrons. The optimized geometry of the transition structure for dissociation from **1a** is shown in Figure 1d. The transition vector²⁰ has two dominant components: the Ge–O distance (0.61 coefficient) and the in-plane HGeO angle (0.62 coefficient); then comes the contribution of the C–O bond, with coefficient -0.32. The main geometrical changes with respect to **1a** which accompany the elongation (by ca. 9%) of the Ge–O bond are a shortening of the C–O bond and a planarization of the formaldehyde moiety, together with a modification of the HGeO angles. These variations go in the direction of the geometries of formaldehyde and germyl anion.²¹ The barrier for dissociation from the carbanion is ca. 10 kcal mol⁻¹. In correspondence of the transition structure, the CI eigenvector is still dominated by the aufbau configuration (0.962 coefficient), but the configuration corresponding to a double excitation from the first into the third active orbital has gained weight (-0.270 coefficient). This results in a depopulation of

(20) The Hessian matrix (frequencies calculation) has been computed in this case numerically, due to memory limitations.

(21) Optimum geometrical parameters (Å, deg) for the heterolytic dissociation limit: C–O = 1.202; C–H = 1.092; \angle HCO = 121.5; Ge–H = 1.691; \angle HGeH = 95.1; for the homolytic dissociation limit: C–O = 1.214; C–H = 1.095; \angle HCO = 122.3; Ge–H = 1.513; \angle HGeH = 120.0.

Table 5. O–Ge Bond Dissociation: Group Charges^a

O–Ge (Å)		Q(CH ₂)		Q(O)		Q(GeH ₃)	
		A	B	A	B	A	B
1.762	1a	-0.472	-0.564	-0.998	-0.641	0.470	0.205
1.80		-0.472	-0.572	-0.977	-0.623	0.450	0.195
1.85		-0.471	-0.578	-0.952	-0.603	0.424	0.181
1.90		-0.467	-0.585	-0.924	-0.577	0.391	0.161
1.917	1d	-0.385	-0.486	-0.865	-0.445	0.250	-0.069
1.95		0.072	-0.111	-0.771	-0.489	-0.301	-0.400
2.00		0.127	-0.114	-0.743	-0.482	-0.385	-0.404
2.05		0.181	-0.117	-0.717	-0.471	-0.464	-0.412
2.10		0.232	-0.117	-0.693	-0.456	-0.539	-0.427
2.15		0.291	-0.109	-0.671	-0.430	-0.620	-0.461

^a Group charges Q computed summing up C and H, or Ge and H, atomic NAO charges (see ref 13) obtained at the HF/[552/331/2] level (column A); at the CAS-MCSCF level, group charges are computed on the basis of Mulliken atomic charges (column B).

the first orbital (1.855 electrons) and a corresponding increase for the third one (0.148); the second one is almost unchanged (1.998).

A series of geometries, which obviously do not belong to critical points, was then obtained by constrained CAS-MCSCF/[552/331/2] optimizations carried out at fixed O–Ge distances, with the aim of getting a qualitatively detailed description of the dissociation process in correspondence of an approximate energy profile. The geometries so obtained evidentiate that significant geometrical changes take place rather abruptly at the transition structure. Not far from the saddle point (O–Ge = 1.90 Å) the two sets of HGeO angles (in-plane and out-of-plane hydrogens) have similar values (110 and 112°), as do HGeH angles (107.4°). All Ge–H bonds have similar lengths (1.55 Å), and the C–O bond is 1.48 Å. All these parameters are still very close to those of the initial carbanion **1a**. In contrast, just beyond the transition structure (O–Ge = 1.95 Å) the HGeO angles are very different (162° the in-plane angle and 94° for the out-of-plane angles), as do the HGeH angles: those involving the in-plane hydrogen are 97.0°, while the other one is 104.8°. Also Ge–H bonds are differentiated: the in-plane Ge–H bond is significantly stretched (1.66 Å), and the others are 1.57 Å. Finally, the C–O bond has shortened to 1.30 Å. These values can be compared with those found for the transition structure **1d**, which are of course in between. The changes in electronic structure at the origin of the features just discussed are reflected also by variations in the group charges: compare for instance, for various O–Ge values, the charge on the germyl group (rightmost B column in Table 5).

The modifications in the nature of the ground state taking place in correspondence of the dissociation process can now be examined. Carrying out for every optimized geometry a CI in terms of the optimized orbitals obtained for the corresponding H₂CO and GeH₃ separated fragments is helpful in analyzing the nature of the polydeterminantal wave function. The ground state of **1a** is dominated by the $\sigma_{\text{OGe}}^2 n_{\text{C}}^2$ configuration, which translates, for the same geometry but in terms of the separate-fragment orbitals, into two covalent configurations (with spin-coupled singly occupied π_{CO} and σ_{GeH_3} , or π^*_{CO} and σ_{GeH_3} orbitals, respectively) and one ionic ($\pi_{\text{CO}}^2 \pi^*_{\text{CO}}^2$, corresponding to an empty σ_{GeH_3} orbital). When dissociation is accomplished, the polarization of the GeH₃ fragment with respect to the H₂CO

counterpart is just the opposite, because it is negatively charged. This is the main modification which occurs in correspondence of the avoided crossing relevant to the dissociation transition structure. While in the ground state of **1a** no configuration with a doubly occupied σ_{GeH_3} fragment orbital gives a significant contribution, a contribution of this kind is present in all remaining higher-energy states. In a parallel fashion, the covalent contribution to the description of **1a** gives a significant contribution to the second electronic state of the separated fragments but not only there. In fact, all electronic states considered in the present computations have the same symmetry and consequently can mix: thus it is not possible to reduce their interplay to a simple two-member mixing in terms of which to interpret the avoided crossing from which the barrier results. It must be noted, however, that in terms of *optimized* orbitals a single configuration always prevails in the CI eigenvector, along the CAS-MCSCF dissociation pathway: its coefficient is close to 0.99 in the part preceding the transition structure, goes down to 0.91 for O–Ge = 1.95 Å, and then up again and is 0.94 at 2.15 Å. This behavior suggests that recomputation of the energies at the (single reference) MP4 level can be not completely unreasonable. This would permit the drawing of an approximate energy plot and the consequent tentative estimate of the energy barrier for dissociation also at this level: this result would be directly comparable with those obtained for the nondissociative process. Therefore, MP4/[552/331/2] calculations were carried out on the geometries obtained by CAS-MCSCF/[552/331/2] optimizations at fixed O–Ge distances. The barrier for dissociation so estimated is ca. 11 kcal mol⁻¹, the highest energy value resulting just in correspondence of the **1d** geometry (Table 3). Again, the change in group charges for the two fragments indicates that the fragments obtained through dissociation are the germyl anion and formaldehyde (Table 5). The MP4 estimate of this dissociation barrier is lower than that obtained for silicon (ca. 30 kcal mol⁻¹),⁶ consistent with the different stability of the dissociation limits with respect to the original carbanions discussed above. Nevertheless it is higher than that the system has to overcome in the nondissociative process, in correspondence with transition structure **1c**; therefore, the dissociation–reassociation pathway does not appear to be significantly competitive.

Even if the reacting system of this kind were inclined to follow in small part a dissociation–reassociation pathway, this result would indicate, incidentally, that radical intermediates are not likely to be involved in the germyl Wright–West migration reaction, in accord with the results obtained for silicon.⁶

Conclusions

The model reactions described in ref 6 and in the present study correspond to an extreme situation of no interaction of the anionic system with the counterion and are strictly pertinent to gas-phase chemistry. However, some important differences in the qualitative description of the two rearrangements originate from the very capability of silicon or germanium to bear a bonding situation with carbon or oxygen or both simultaneously. Therefore, the present results can be thought of as being of some relevance to solution chemistry too.

In both cases ($X = \text{Si}, \text{Ge}$) the direct XH_3 [1,2] migration pathway passes through a zone in which a cyclic pentacoordinate-X structure is present. While in the case of silicon a real intermediate is involved in the process, in the case of germanium only a flat zone of the hypersurface is defined (shoulder) and a cyclic structure is unstable with respect to the final oxyanion. Comparison of the energy differences between the cyclic structures and the relevant initial and final open-chain structures suggest that germanium is not as inclined as silicon to give a stable pentacoordinated cyclic arrangement. In conclusion, proton abstraction from a germyl ether is expected, on the basis of the present results, to induce a rapid transformation of the initial open-chain carbanionic structure into the final open-chain oxyanion. The initial carbanion will then be

virtually absent when the system will be eventually exposed to the action of a protonating agent or to any other electrophile. The silicon system, on the other hand, could react with some involvement of the cyclic intermediate, with ring opening and cleavage of either the C-Si or O-Si bonds.

Acknowledgment. Financial support from the Italian MURST and from the Italian CNR (within the project "Progetto Strategico Tecnologie Chimiche Innovative") is gratefully acknowledged. Some computations were carried out on an IBM RISC-6000/550 computer provided by the Italian CNR within the project "Calcolo Avanzato in Chimica".

OM9504819